Proton controlled intramolecular communication in dinuclear ruthenium(II) polypyridine complexes

Pietro, Cinzia Di; Serroni, Scolastica; Campagna, Sebastiano; Gandolfi, Maria Teresa; Ballardini, Roberto; Fanni, Stefano; Browne, Wesley R.; Vos, Johannes G.

Published in:
Inorganic Chemistry

DOI:
10.1021/ic0112894

Publication date:
2002

Inorg. Chem. **2002**, *41*, 2871–2878

Proton Controlled Intramolecular Communication in Dinuclear Ruthenium(II) Polypyridine Complexes

Cinzia Di Pietro,[†] Scolastica Serroni,[†] Sebastiano Campagna,[†] Maria Teresa Gandolfi,[‡] Roberto Ballardini,[‡] Stefano Fanni,[§] Wesley R. Browne,[§] and Johannes G. Vos*[,§]

Dipartimento di Chimica Inorganica, Chimica Analitica e Chimica Fisica dell'Università, Via Sperone 31, I-98166 Messina, Italy, Dipartimento di Chimica, "G. Ciamician", Via Selmi 2, I-40126 Bologna, Italy, and National Centre for Sensor Research, School of Chemical Science, Dublin City University, Dublin 9, Ireland

Received December 18, 2001

The synthesis and characterization of two dinuclear ruthenium polypyridyl complexes based on the bridging ligands 5,5′-bis(pyridin-2″-yl)-3,3′-bis(1H-1,2,4-triazole) and 5,5′-bis(pyrazin-2″-yl)-3,3′-bis(1H-1,2,4-triazole) and of their mononuclear precursors are reported. The dinuclear compounds have been prepared by a Ni(0) catalyzed coupling of a mononuclear ruthenium(II) polypyridyl complex containing a brominated triazole moiety. Electrochemical and photophysical studies indicate that, in these dinuclear complexes, the protonation state of the bridge may be used to tune the intercomponent interaction between the two metal centers and that these species act as proton driven three-way molecular switches that can be read by electrochemical or luminescence techniques.

Introduction

Ruthenium(II) polypyridine complexes are playing a key role for the development of multicomponent (supramolecular) systems capable of performing photo- and/or redox-triggered functions. Examples are artificial antenna systems,[1] charge separation devices for photochemical solar energy conversion,[1] and information storage devices.[2] Of particular interest in this regard are molecular components with well-defined photophysical and redox properties, which can be switched or tuned by external perturbation.[3]

For the past number of years, there has been considerable interest in the study of mononuclear and multinuclear ruthenium(II) polypyridyl complexes containing ligands such as 3,5-bis(pyridin-2′-yl)-1H-1,2,4-triazole (Hbpt)[4] and 3,5-bis(pyrazin-2′-yl)-1H-1,2,4-triazole) (Hbpzt)[5] (Figure 1). It has been shown that for dinuclear compounds featuring these ligands strong interaction is observed between metal centers.[6]

In this contribution, the syntheses and spectroscopic, photophysical, and redox properties of two new dinuclear ruthenium(II) complexes $[(bpy)_2Ru(bpbt)Ru(bpy)_2]^{2+}$ (**1**) (where H_2bpbt is 5,5′-bis(pyridin-2″-yl)-3,3′-bis(1H-1,2,4-triazole)) and $[(bpy)_2Ru(bpzbt)Ru(bpy)_2]^{2+}$ (**2**) (where H_2-

* Corresponding author. E-mail: johannes.vos@dcu.ie. Fax: 00353 1 7005503. Phone: 00353 1 700 5307.
[†] Chimica Analitica e Chimica Fisica dell'Università.
[‡] "G. Ciamician".
[§] Dublin City University.

(1) (a) Balzani, V.; Juris, A.; Venturi, M.; Campagna, S.; Serroni, S. *Acc. Chem. Res.* **1998**, *31*, 26. (b) Slate, C. A.; Striplin, D. R.; Moss, J. A.; Chen, P.; Erickson, B. W.; Meyer, T. J. *J. Am. Chem. Soc.* **1998**, *120*, 4885. (c) Hu, Y.-Z.; Tsukiji, S.; Shinkai, S.; Oishi, S.; Hamachi, I. *J. Am. Chem. Soc.* **2000**, *122*, 241. (d) Balzani, V.; Juris, A.; Venturi, M.; Campagna, S.; Serroni, S. *Chem. Rev.* **1996**, *96*, 759.

(2) (a) Juris, A.; Balzani, V.; Barigelletti, F.; Campagna, S.; Belser, P.; von Zelewsky, A. *Coord. Chem. Rev.* **1988**, *84*, 85. (b) Meyer, T. J. *Acc. Chem. Res.* **1989**, *22*, 163. (c) O'Regan, B.; Graetzel, M. *Nature* **1991**, *335*, 737. (d) De Cola, L.; Belser, P. *Coord. Chem. Rev.* **1998**, *177*, 301. (e) Bignozzi, C. A.; Schoonover, J. R.; Scandola, F. *Prog. Inorg. Chem.* **1997**, *44*, 1. (f) Blanco, M.-J.; Jiménez, M. C.; Chambron, J.-C.; Heitz, V.; Linke, M.; Sauvage, J.-P. *Chem. Soc. Rev.* **1999**, *28*, 293.

(3) (a) Beer, P. D.; Szemes, F.; Balzani, V.; Salà, C. M.; Drew, M. G.; Dent, S. W.; Maestri, M. *J. Am. Chem. Soc.* **1997**, *119*, 11864. (b) Barigelletti, F.; Flamigni, L.; Collin, J.-P.; Sauvage, J.-P. *Chem. Commun.* **1997**, 333. (c) Waldmann, O.; Hassmann, J.; Müller, P.; Hanan, G. S.; Volkmer, D.; Schubert, U. S.; Lehn, J.-M. *Phys. Rev. Lett.* **1997**, *78*, 3390. (d) Zahavy, E.; Fox, M. A. *Chem.—Eur. J.* **1998**, *4*, 1647. (e) Balzani, V.; Credi, A.; Venturi, M. *Curr. Opin. Chem. Biol.*, **1997**, *1*, 506.

(4) (a) Hage, R.; Prins, R.; Haasnoot, J. G.; Reedijk, J.; Vos, J. G. *J. Chem. Soc., Dalton Trans.* **1987**, 1389. (b) Nieuwenhuis, H. A.; Haasnoot, J. G.; Hage, R.; Reedijk, J.; Snoeck, T. L.; Stufkens, D. J.; Vos, J. G. *Inorg. Chem.* **1990**, *30*, 48. (c) Buchanan, B. E.; Wang, R.; Vos, J. G.; Hage, R.; Haasnoot, J. G.; Reedijk, J. *Inorg. Chem.* **1990**, *29*, 3263. (d) Browne, W. R.; O'Connor, C. M.; Villani, C.; Vos, J. G. *Inorg. Chem.* **2001**, *40*, 5461. (e) Wang, R.; Vos, J. G.; Schmehl, R. H.; Hage, R.; *J. Am Chem. Soc.* **1992**, *114*, 1964.

(5) (a) Hage, R.; Dijkhuis, A. H. J.; Haasnoot, J. G.; Prins, R.; Reedijk, J.; Buchanan, B. E.; Vos, J. G. *Inorg. Chem.* **1988**, *27*, 2185. (b) Barigelletti, F.; De Cola, L.; Balzani, V.; Hage, R.; Haasnoot, J. G.; Vos, J. G. *Inorg. Chem.* **1989**, *28*, 4344.

(6) Hage, R.; Haasnoot, J. G.; Nieuwenhuis, H. A.; Reedijk, J.; De Ridder, D. J. A.; Vos, J. G. *J. Am. Chem. Soc.* **1990**, *112*, 9249.

10.1021/ic0112894 CCC: $22.00
Published on Web 04/30/2002

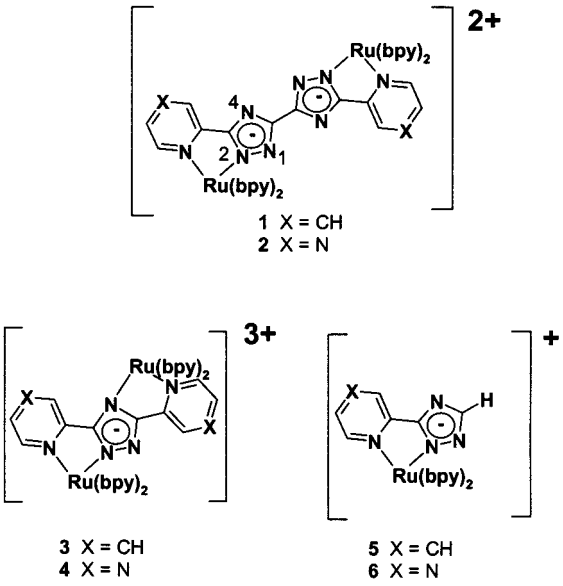

Figure 1. Complex structures.

bpzbt = 5,5′-bis(pyrazin-2″-yl)-3,3′-bis(1H-1,2,4-triazole)) are reported, together with the synthesis and characterization of their mononuclear precursors. The structures of **1** and **2**, of the dinuclear compounds $[(Ru(bpy)_2)_2(bpt)]^{3+}$ (**3**) and $[(Ru(bpy)_2)_2(bpzt)]^{3+}$ (**4**), and of some other mononuclear analogues, used for comparison, are shown in Figure 1.

A first feature of this study is the manner in which the title compounds have been synthesized. The N2 and N4 coordination sites of the triazole ring are nonequivalent,[7] and direct synthesis of the dinuclear species from the bridging H_2bpbt and H_2bpzbt ligands leads in our hands to the formation of an ill defined mixture of products. Possible isomers are shown in Figure 2. The dinuclear compounds have been prepared by a Ni(0) catalyzed homonuclear coupling of a bromine substituted ruthenium(II) polypyridyl complex. With this synthetic method, a single well-defined product is obtained.

The second purpose is the investigation of the intercomponent processes in **1** and **2** as a function of the protonation state of the bridging ligand. The important observation is that by control of the protonation of the bridge a three-way proton controlled molecular switch is obtained, which can be read by electrochemical or spectroscopic methods. A preliminary communication on this work has recently appeared.[8]

Experimental Section

Materials. All solvents used for spectroscopic measurements were of Uvasol (Merck) grade. All other reagents were HPLC grade or better. *cis*-$[Ru(bpy)_2Cl_2]\cdot 2H_2O$ was prepared by standard procedures.[9] Complexes **3**−**6** have been prepared by previously reported procedures.[4−7]

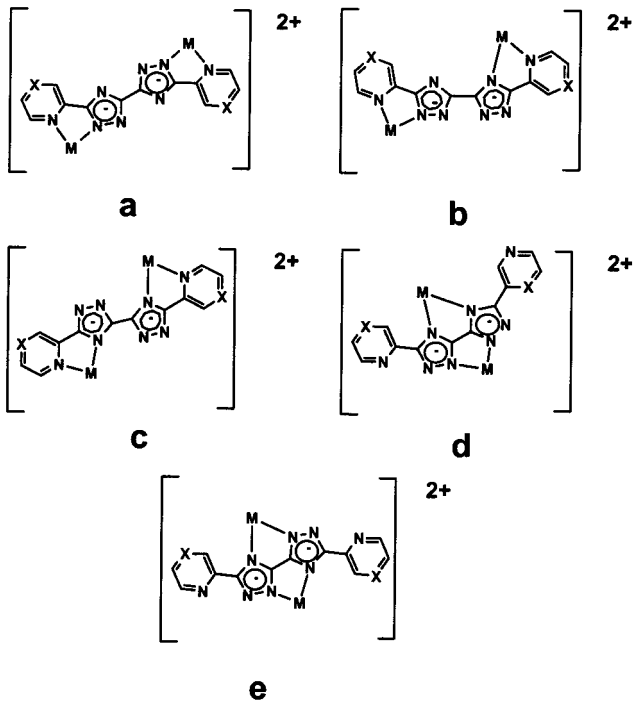

Figure 2. Possible coordination isomers formed by direct reaction of H_2-bpbt or H_2bpzbt with *cis*-$[Ru(bpy)_2Cl_2]$ (X = CH or N).

Synthetic Methods. 3-Bromo-5-(pyridin-2′-yl)-1H-1,2,4-triazole (HBrpytr). A suspension of 3-(pyridin-2′-yl)-1H-1,2,4-triazole (880 mg, 6 mmol) in H_2O (15 mL) was dissolved by slow addition of 10 M NaOH (pH ∼ 12). Subsequently, 0.6 mL of Br_2 (99%; d = 3.199 g/mL) was added slowly while maintaining a pH of 12 by addition of concentrated NaOH solution. After stirring for 3 h, the solution was acidified to pH 3−4 with 5 M HCl (aq), resulting in precipitation of the brominated ligand, which was collected by suction filtration. Yield: 945 mg (70%). ^{1}H NMR data d_6-DMSO: H3, 8.60 ppm (d); H4, 7.85 ppm (t); H5, 7.49 ppm (t); H6, 8.00 ppm (d).

3-Bromo-5-(pyrazin-2′-yl)-1H-1,2,4-triazole (HBrpztr). This compound was obtained from 3-(pyrazin-2-yl)-1H-1,2,4-triazole using the method described for HBrpytr. Yield: 920 mg (65%). ^{1}H NMR data *d*-chloroform: H3, 9.40 ppm (s); H5, 8.72 ppm (d); H6, 8.65 ppm (d).

$[Ru(bpy)_2(Brpytr)]PF_6\cdot H_2O$. A suspension of HBrpytr (200 mg, 0.9 mmol) and *cis*-$[Ru(bpy)_2Cl_2]\cdot 2H_2O$ (348 mg, 0.67 mmol) in 20 mL of EtOH/H_2O (1:1, v/v) was heated at reflux for 2 h. After cooling to room temperature, the reaction mixture was filtered and reduced in volume in vacuo. Two drops of a 30% NH_4OH solution were added prior to addition of saturated aqueous solution of NH_4-PF_6 (3 mL) to induce precipitation. The solid was separated by vacuum filtration and washed with 20 mL of diethyl ether. The red-orange product was obtained in a pure form by recrystallization from acetone/water (1:1, v/v). Yield: 59%. ^{1}H NMR data d_3-acetonitrile: 7.15 ppm (dd, 1H), 7.30 ppm (dd, 1H), 7.42 ppm (dd, 2H), 7.51 ppm (dd, 1H), 7.59 ppm (d, 1H), 7.70 ppm (d, 1H), 7.83 ppm (d, 1H), 7.85 ppm (dd, 1H), 7.9 ppm (m, 3H), 7.99 ppm (m, 3H), 8.03 ppm (dd, 1H), 8.52 ppm (dd, 1H), 8.56 ppm (d, 1H), 8.6 ppm (dd, 2H). UV−vis absorption spectroscopy: λ_{max} = 475 nm (ϵ = 11600 M^{-1} cm^{-1}). Luminescence spectroscopy: λ_{max} = 665 nm, τ = 250 ns at 298 K in deaerated acetonitrile. Acid/base properties: pK_a 1.3, pH_i 0.9. Anal. Calcd for $C_{27}H_{22}OBrF_6N_8PRu$: C, 40.50%; H, 2.75%; N, 14.06%. Found: C, 40.79%; H, 2.57%; N, 13.94%. Mass spectroscopy: molecular$^+$ ion (for $C_{27}H_{20}N_8$-

(7) (a) Niewenhuis, H. A.; Haasnoot, J. G.; Hage, R.; Reedijk, J.; Snoeck, T. L.; Stufkens, D. J.; Vos, J. G. *Inorg. Chem.* **1991**, *30*, 48. (b) Fanni, S.; Keyes, T. E.; O'Connor, C. M.; Hughes, H.; Wang, R.; Vos, J. G. *Coord. Chem. Rev.* **2000**, *208*, 77.
(8) Fanni, S.; Di Pietro, C.; Serroni, S.; Campagna, S.; Vos, J. G. *Inorg. Chem. Commun.* **2000**, *3*, 42.
(9) Sullivan, B. P.; Salmon, D. J.; Meyer, T. J. *Inorg. Chem.* **1978**, *17*, 3334.

$RuBr^+$) at 637/639 *m*/*z* units ($^{79}Br/^{81}Br$). The isotopic pattern is in agreement with theoretical values.

[Ru(bpy)$_2$(Brpztr)]PF$_6$·H$_2$O. *cis*-[Ru(bpy)$_2$Cl$_2$]·2H$_2$O (519 mg, 0.67 mmol) with 300 mg (0.9 mmol) of HBrpztr was heated at reflux in 20 mL of EtOH/H$_2$O (1:1, v/v) for 3 h. The pure complex was obtained using the method described for [Ru(bpy)$_2$(Brpytr)]-PF$_6$·H$_2$O. Yield: 64%. ^{1}H NMR d_3-acetonitrile: 7.35 ppm (dd, 1H), 7.41 ppm (dd, 1H), 7.45 ppm (dd, 1H), 7.53 ppm (dd, 1H), 7.71 ppm (d, 1H), 7.76 ppm (d, 1H), 7.83 ppm (d, 1H), 7.9 ppm (m, 3H), 8.06 ppm (m, 3H), 8.22 ppm (d, 1H), 8.58 ppm (dd, 2H), 8.65 ppm (dd, 2H), 9.02 ppm (d, 1H). UV−vis absorption spectroscopy: $\lambda_{max} = 450$ nm ($\epsilon = 12900$ M^{-1} cm^{-1}). Luminescence spectroscopy: $\lambda_{max} = 647$ nm, $\tau = 200$ ns at 298 K in deaerated acetonitrile. Acid/base properties: pK_a 1.4, pH$_i$ 1.1/5.5. Anal. Calcd for $C_{23}H_{21}OBrF_6N_9PRu$: C, 39.00%; H, 2.62%; N, 15.73%. Found: C, 39.47%; H, 2.69%; N, 15.24%. Mass spectroscopy: molecular$^+$ ion (for $C_{26}H_{19}N_9RuBr^+$) at 638/640 *m*/*z* units ($^{79}Br/^{81}Br$). The isotopic pattern is in agreement with theoretical values.

[{Ru(bpy)$_2$}$_2$bpbt](PF$_6$)$_2$·4H$_2$O (1). In a 5 mL round-bottomed, two-necked flask equipped with magnetic stir bar and rubber septum were placed 124 mg (0.524 mmol) of NiCl$_2$·6H$_2$O and 549 mg (2.1 mmol) of PPh$_3$. The flask was purged with nitrogen prior to addition of dry DMF (2 mL) via a syringe. The blue reaction mixture was stirred at room temperature, under nitrogen, for 30 min followed by addition of 33 mg (0.524 mmol) of zinc powder. To the dark-brown catalyst formed (1 h, under nitrogen) was added 410 mg (0.524 mmol) of [(bpy)$_2$Ru(Brpytr)]PF$_6$·H$_2$O, and the resulting mixture was heated at 95 °C for 4 h. After the reaction mixture cooled to room temperature, Et$_2$O was added to induce precipitation; the crude product so obtained was dissolved in acetone/water (1:1, v/v) with 2 drops of 30% NH$_4$OH and 3 mL of a saturated aqueous solution of NH$_4$PF$_6$. The product was separated by filtration, dissolved in a small volume of MeCN/MeOH (50:1, v/v), and purified by chromatography on neutral alumina with MeCN/MeOH (50:1, v/v). The second red-orange band was collected, and the solvent was evaporated under reduced pressure. The deep-red product obtained was recovered by filtration and was purified by recrystallization from acetone/water (1:1, v/v). Yield: 40%. Anal. Calcd for $C_{54}H_{48}O_4F_{12}N_{16}P_2Ru_2$: C, 43.91%; H, 3.28%; N, 15.17%. Found: C, 44.21%; H, 3.32%; N, 15.56%. Mass spectroscopy: *m*/*z* 558 (M^{2+} ion calculated for $C_{54}H_{40}N_{16}Ru_2^{2+}$: 558). ^{1}H NMR data ($d_6$-acetone) δ ppm: 8.73 (dd, 4H), 8.64 (m, 4H), 8.07 (m, 12H), 7.95 (dd, 2H), 7.87 (dd, 2H), 7.64 (d, 2H), 7.52 (m, 6H), 7.40 (dd, 2H), 7.36 (dd, 2H), 7.19 (dd, 4H).

[{Ru(bpy)$_2$}$_2$bpzbt](PF$_6$)$_2$.4H$_2$O (2). This complex was obtained using the method described for **1**. Yield: 50%. Anal. Calcd for $C_{52}H_{46}O_4F_{12}N_{18}P_2Ru_2$: C, 42.22%; H, 3.11%; N, 17.05%. Found: C, 42.80%; H, 2.75%; N, 16.80%. Mass spectroscopy: 559 *m*/*z* units (M^{2+} ion calculated for $C_{52}H_{38}N_{18}Ru_2^{2+}$: 559).^{1}H NMR data ($d_6$-acetone/NaOD) δ ppm: 9.3 (d, 1H), 9.25 (d, 1H), 8.76 (dd, 4H), 8.67 ppm (dd, 4H), 8.31 (d, 2H), 8.10 (m, 8H), 7.92 (dd, 2H), 7.85 (dd, 2H), 7.82 (dd, 2H), 7.56 (m, 4H), 7.44 (m, 8H).

Instrumentation. ^{1}H NMR spectra were recorded on a Bruker AC400 (400 MHz) NMR spectrometer. All measurements were carried out in d_6-DMSO or *d*-chloroform for ligands and in d_6-acetone for complexes. Peak positions are relative to residual solvent peaks. UV−vis absorption spectra were recorded on a Shimadzu UV−vis−NIR 3100 spectrophotometer interfaced with an Elonex PC466 using UV−vis data manager. Absorption maxima are ±2 nm; molar absorption coefficients are ±10%. Emission spectra (accuracy ±5 nm) were recorded at 298 K using an LS50B luminescence spectrophotometer, equipped with a red sensitive Hamamatsu R928 PMT detector, interfaced with an Elonex PC466 employing Perkin-Elmer Fl WinLab custom built software. Emission spectra are uncorrected for photomultiplier response. Quartz cells (10 mm path length) were used. Emission quantum yields were measured at room temperature with the optically dilute method using $[Ru(bpy)_3]^{2+}$ in aerated aqueous solution as a quantum yield standard, assuming a value of 0.028,[10,11] and are ±10%. pH titrations of **1** and **2** were carried out in Britton−Robinson buffer (0.04 M H_3BO_3, 0.04 M H_3PO_4, 0.04 M CH_3CO_2H) (pH was adjusted using concentrated sulfuric acid or sodium hydroxide solution). pH$_i$ refers to the inflection point of the emission titration curve. The appropriate isobestic point from the absorption spectra was used as the excitation wavelength for emission titrations.

Luminescence lifetime measurements were obtained using an Edinburgh Analytical Instruments (EAI) time-correlated single-photon counting apparatus (TCSPC) composed of two model J-yA monochromators (emission and excitation), a single photon photomultiplier detection system model 5300, and a F900 nanosecond flashlamp (N_2 filled at 1.1 atm pressure, 40 kHz), interfaced with a personal computer via a Norland MCA card. A 500 nm cut off filter was used in emission to attenuate scatter of the excitation light (337 nm). Data correlation and manipulation were carried out using EAI F900 software version 5.1.3. Samples were deaerated for 20 min using Ar gas before measurements were carried out. In the case of complex **2**, samples were deaerated via three freeze−pump−thaw cycles. Emission lifetimes were calculated using a single-exponential fitting function; a Levenberg−Marquardt algorithm with iterative reconvolution Edinburgh instruments F900 software was used; uncertainty is ±10%. The reduced χ^2 and residual plots were used to judge the quality of the fits.

Mass spectra were obtained using a Bruker-Esquire LC 00050 electrospray ionization mass spectrometer at positive polarity with cap-exit voltage of 167 V. Spectra were recorded in the scan range 50−2200 *m*/*z* with an acquisition time of between 300 and 900 μs and a potential of between 30 and 70 V. Each spectrum was recorded by summation of 20 scans.

Elemental analysis has been carried out at the Microanalytical Laboratory at University College Dublin.

Electrochemical measurements were carried out on a Model 660 electrochemical workstation (CH Instruments). Typical complex concentrations were 0.5−1 mM in anhydrous acetonitrile containing 0.1 M tetraethylammonium perchlorate (TEAP). A Teflon shrouded glassy carbon working electrode, a Pt wire auxiliary electrode, and an SCE reference electrode were employed. Solutions for reduction measurements were deoxygenated by purging with N_2 or Ar gas for 15 min prior to the measurement. Measurements were made in the range −2.0 to 2.0 V versus SCE. Protonation of complexes was achieved by addition of 0.1 M trifluoromethanesulfonic acid in acetonitrile. pH cyclic voltammograms were obtained at sweep rates of 20, 50, 200, and 500 mV s^{-1}; differential pulse voltammetry (DPV) experiments were performed with a scan rate of 20 mV s^{-1}, a pulse height of 75 mV, and a duration of 40 ms. For reversible processes, the half-wave potential values are reported; identical values are obtained from DPV and CV measurements. Redox potentials are ±10 mV. Spectroelectrochemistry was carried out using an OTTLE setup composed of a homemade Pyrex glass, thin layer cell (2 mm). The optically transparent working electrode was made from platinum−rhodium gauze, a platinum wire counter electrode, and the reference electrode, which was a pseudo-Ag/AgCl reference electrode. The working electrode was held at the

(10) Demas, J. N.; Crosby, G. A. *J. Phys. Chem.* **1971**, *75*, 991.
(11) Nakamaru, N. *Bull. Chem. Soc. Jpn.* **1982**, *55*, 2697.

Table 1. Electronic, Photophysical, and Redox Data for Complexes **1**−**6**[a]

		absorption λ_{max}[b] nm	emission, 298 K λ_{max}[b] nm, (τ, ns) {Φ*10^{-3}}	E (ox) V vs SCE
1	$[(bpy)_2Ru(bpbt)Ru(bpy)_2]^{2+}$	480	690 (102) {2.4}	+0.80 [1], +0.98 [1]
H1	$[(bpy)_2Ru(Hbpbt)Ru(bpy)_2]^{3+}$	440	660 (344) {2.1}	+1.06 [1], +1.17 [1]
$H_2$1	$[(bpy)_2Ru(H_2bpbt)Ru(bpy)_2]^{4+}$	431	630 (<5 ns)	+1.10 [2]
3	$[(bpy)_2Ru(bpt)Ru(bpy)_2]^{3+}$	452	648 (80)	+1.04 [1], +1.34 [1]
5	$[(bpy)_2Ru(pytr)]^{+}$	467	650 (145)	+0.83 [1]
H5	$[(bpy)_2Ru(Hpytr)]^{2+}$	438	612 (<1 ns)	+1.14[1]
2	$[(bpy)_2Ru(bpzbt)Ru(bpy)_2]^{2+}$	455	670 (214) {3.4}	+0.92 [1], +1.09 [1]
H2	$[(bpy)_2Ru(Hbpzbt)Ru(bpy)_2]^{3+}$	436	675 (764)	+1.09 [1], +1.15 [1]
$H_2$2	$[(bpy)_2Ru(H_2bpzbt)Ru(bpy)_2]^{4+}$	430	678 (1000) {7.2}	+1.13 [2]
4	$[(bpy)_2Ru(bpzt)Ru(bpy)_2]^{3+}$	449	690 (106)	+1.16 [1], +1.46 [1]
6	$[(bpy)_2Ru(pztr)]^{2+}$	458	660 (250)	+1.01 [1]
H6	$[(bpy)_2Ru(Hpztr)]^{2+}$	441	665 (430)	+1.25[1]
	$[Ru(bpy)_3]^{2+}$	452	620 (1000)	+1.26 [1]

[a] Bracketed numbers ([ ]) refer to the number of electrons under the wave. [b] In acetonitrile at 298 K. Data for the mononuclear pyridine and pyrazine model compounds $[Ru(bpy)_2(pytr)]^{2+}$ (**5**) and $[Ru(bpy)_2(pztr)]^{2+}$ (**6**), respectively, (where Hpytr = 3-(pyridin-2′-yl)-1H-1,2,4-triazole and Hpztr = 3-(pyrazin-2′-yl)-1H-1,2,4-triazole) are included for comparison.

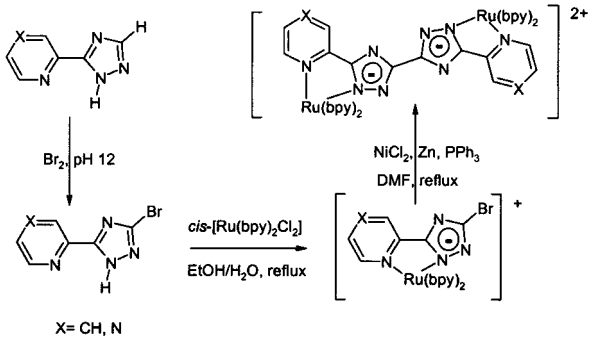

Figure 3. Synthetic scheme employed in preparation of **1** and **2**.

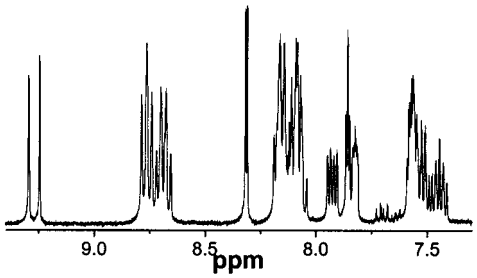

Figure 4. ^{1}H NMR spectra of **2** in d_3-acetone.

required potential throughout the measurement using an EG&G PAR Model 362 potentiostat. Absorption spectra were recorded as described previously. Protonation of complexes under bulk electrolysis was achieved by the addition of a dry 1 M trifluoroacetic acid solution in acetonitrile.

Results

General. The approach taken in this study to obtain pure, well-defined products is outlined in Figure 3. The synthesis of the brominated precursors has been carried out following procedures normally applied to the synthesis of triazole containing ruthenium(II) polypyridyl complexes.[4,5] The mono- and diprotonated complexes of **1** and **2**, which are produced in situ by the addition of an appropriate amount of triflic acid, are referred to as **H1**/**H2** and **$H_2$1**/**$H_2$2**, respectively. The materials obtained from this approach have been fully characterized using spectroscopic measurements. The ^{1}H NMR spectral data shown in Figure 4 illustrate the symmetric nature of the complexes. Spectral assignments are given in the Experimental Section.

Photophysical Properties. All spectroscopic data for complexes **1** and **2** are presented in Table 1, together with data for model complexes **3**−**6**. The absorption spectra of complexes **1** and **2** show intense bands in the UV region [**1**, λ_{max} = 243 nm (ϵ = 52500 M^{-1} cm^{-1}), 290 nm (ϵ = 124100 M^{-1} cm^{-1}); **2**, 244 nm (ϵ = 53400 M^{-1} cm^{-1}), 288 nm (ϵ = 126600 M^{-1} cm^{-1})] and moderately intense bands in the visible region [(**1**, 480 nm (ϵ = 17400 M^{-1} cm^{-1}); **2**, 455 nm (ϵ = 25400 M^{-1} cm^{-1})], which are typical for these types of complexes.[4,5] The complexes are luminescent in acetonitrile at 298 K, and excitation spectra match closely the absorption spectra. Luminescence lifetimes at room temperature are strictly single exponential and are in the 100−1000 ns time domain. Luminescence quantum yields at room temperature are of the order of 10^{-3} (Table 1).

Acid−**Base Properties.** The spectroscopic, photophysical, and redox properties (vide infra) of **1** and **2** are dependent on the protonation state of the complex. For **1**, in aqueous buffered solution, UV−vis spectroscopy as a function of pH yields two reversible protonation steps with pK_a values of 1.1 and 3.8. On the basis of former protonation studies on Ru(II) complexes containing triazolate ligands,[12] the protonation processes can be attributed to protonation of the triazole rings. However, the two successive pK_a values obtained suggest that the triazole rings interact and the monoprotonated species is better viewed as a compound where the added proton is shared between the two triazole units of the bridging ligand. As with the structurally similar mononuclear complexes **5** and **6**, protonation results in a blue shift in the UV−vis absorption spectra. Complex **2**, as observed for **6**, shows only minor changes in its UV−vis spectra upon protonation, and hence, reliable determination of pK_a values is not possible. For **2**, additional protonation states exist via protonation of pyrazine; however, such protonation occurs only at very negative pH and need not be considered in the pH range studied.[7]

The emission properties of **1** and **2** also show pH dependence (see Table 1). Emission spectra obtained for **1**

(12) (a) Vos, J. G. *Polyhedron* **1992**, *11*, 2285. (b) Hossain, Md. D.; Ueno, R.; Haga, M. *Inorg. Chem. Commun.* **2000**, *3*, 35. (c) Haga, M.; Ali, Md. M.; Maegawa, H.; Nozaki, K.; Yoshimura, A.; Ohno, T. *Coord. Chem Rev.* **1994**, *132*, 99.

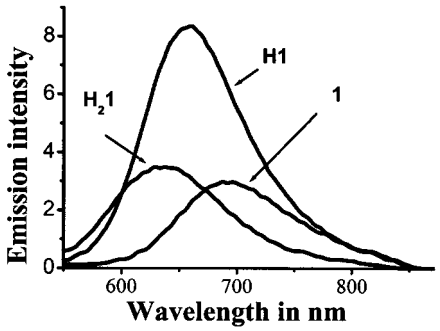

Figure 5. Emission spectra of **1**, **H1**, and $\mathbf{H_2 1}$ in acetonitrile (protonation with CF_3SO_3H acid).

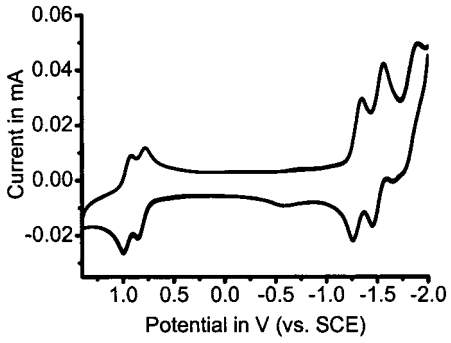

Figure 6. Cyclic voltammogram of **1** in acetonitrile solution.

at three different protonation states are shown in Figure 5. The emission spectrum of **1** undergoes a blue shift from 690 nm (**1**) to 660 nm (**H1**) to 630 nm ($\mathbf{H_2 1}$) in acetonitrile. The inflection points of the emission titration curves (pH_i) are observed at pH 0.45 and 2.7 in buffered aqueous solution (see Experimental Section). Single protonation of **1** to **H1** results in an increase of emission lifetime, in contrast with the effect of the protonation of the mononuclear complex **5**. However, the doubly protonated complex $\mathbf{H_2 1}$ compares well in terms of emission energy and emission lifetime with **H5**.

For **2**, protonation results in a small red shift in the emission spectrum (~10 nm) in agreement with similar pyrazine based complexes (e.g., **6**/**H6**).[13] Compared with **1**, the changes in emission energy are much smaller, but the emission lifetime of the emitting state increases with each protonation step. It should be noted that protonation of the pyrazine ring in the exited state is easier than in the ground state. For **H6**/$\mathbf{H_2 6}$, a pH_i value of 2.0 has been reported. Because this process leads to quenching of the emission, the acidity of the measuring solution needs to be controlled carefully.

Redox Properties. The metal based oxidation potentials for **1** and **2** and for their protonated forms together with those of the model compounds are collected in Table 1. Both **1** and **2** undergo several reversible oxidation and reduction processes within the redox window investigated (between +2.0 and −2.0 V vs SCE) (see Figure 6). For both **1** and **2**, the first metal oxidation potential is close to that of monomers **5** and **6**, respectively, and at lower potential than those of dinuclear complexes **3** and **4**. For both **1** and **2**, an increase

(13) Hage, R.; Haasnoot, J. G.; Nieuwenhuis, H. A.; Reedijk, J.; Wang, R.; Vos, J. G. *J. Chem. Soc., Dalton Trans.* **1991**, 3271.

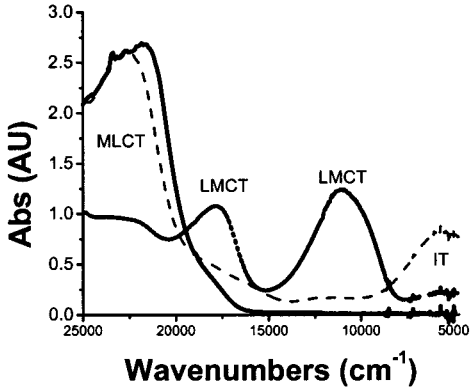

Figure 7. Visible and near-IR absorption spectra of **2** in acetonitrile with 0.1 TEAP at 0.60 V (solid line), 1.00 V (dashed line), and 1.10 V (dotted line) vs SCE.

in the metal based oxidation potentials is observed upon protonation, together with a significant decrease in the gap between the first and second oxidation waves, from ~135 mV for both **1** and **2** to less than 70 mV for **H1** and **H2**. Both $\mathbf{H_2 1}$ and $\mathbf{H_2 2}$ exhibit a single two electron metal oxidation wave at potentials comparable to those observed for **H5** and **H6**. The ligand based reduction processes are as expected for ruthenium polypyridyl complexes and are not further discussed.[4,5]

Spectroelectrochemistry. The visible−near-infrared spectra of **2**, of the electrochemically generated mixed valence and fully oxidized species, are shown in Figure 7. Only minor differences are observed in the energy of the intervalence (IT) and ligand-to-metal-charge-transfer (LMCT) bands in **1** and **2** and in **H1** and **H2**. For **1** and **2**, the formation of the mixed valence species is identified by a decrease in the intensity of the ^{1}MLCT bands at ~22220 cm^{-1} (450 nm) and the formation of new bands at ~5500 cm^{-1} and at 11000 and 17500 cm^{-1}. Bulk electrolysis at a potential above the second oxidation wave results in the complete depletion of the 22220 cm^{-1} band coupled with a concomitant depletion of the band at 5500 cm^{-1} and a further increase in both bands at 11000 and 17500 cm^{-1}. All processes are fully reversible.

Reversible spectroelectrochemistry is also observed for **H1** and **H2**. For both compounds, after applying a potential of 1.2 V (vs pseudo-Ag/AgCl), the formation of a band at about 8700 cm^{-1} is observed; further increase of the potential past the second oxidation potential of the complex results in the formation of spectral features at 17860 and 11175 cm^{-1} with concomitant depletion of the band at 8700 cm^{-1}. However, analysis of the IT bands is difficult, because they are located in an area of the spectrum where both LMCT and IT bands are expected. For the fully protonated complexes $\mathbf{H_2 1}$ and $\mathbf{H_2 2}$, no evidence for intervalence bands was found. However, in the presence of triflic acid, the fully oxidized $\mathbf{H_2 1}$ and $\mathbf{H_2 2}$ exhibit spectral features, most likely LMCT bands at 23360 and 12550 cm^{-1} that are, however, less intense and blue-shifted with respect to those of the mono- and deprotonated species.

Discussion

Synthesis and Characterization. As pointed out in the Introduction, the preparation of complexes with ligands such

as H_2bpbt and H_2bpzbt is by no means straightforward. Because the N2 and N4 nitrogen atoms of the triazole ring are chemically nonequivalent, direct synthesis of the complexes from these ligands can yield five possible coordination isomers, on the basis of the binding mode of the five-membered ring (Figure 2). In three of these isomers (isomers **a**−**c** in Figure 2), the $Ru(bpy)_2$ moiety is bound to a pyridine (or pyrazine) and a triazole ring; in the other two isomers, coordination takes place via the two central triazole rings and does not involve the pyridine and pyrazine rings (isomers **d** and **e** in Figure 2).[14] To avoid the formation of so many different coordination isomers, a new synthetic method was developed.[8] This method is based on the Ni(0) catalyzed coupling reported for bromide containing organic compounds.[15]

In this synthetic approach, brominated pyridine and pyrazine triazole ligands were prepared by adapting procedures previously reported for the bromination of 1,2,4-triazoles.[16] These brominated ligands were subsequently complexed with *cis*-$[Ru(bpy)_2Cl_2]\cdot 2H_2O$, and the products obtained from this complexation reaction were reacted with Ni(0) to produce the dinuclear complexes. With this method, the formation of complexes where the metal centers are coordinated to the two central triazole rings is prevented.

As already noted, the N2 and N4 coordination sites of the triazole ring (see Figure 2) are not equivalent, and therefore, the formation of coordination isomers is expected.[7] The introduction of the bromine atom, although primarily for use in the coupling reaction, has the secondary effect that the presence of this bulky atom in the 3-position results in the formation of the N2 isomer (>95%) over the N4 isomer (<5%), with the N4 isomer being lost during subsequent recrystallization. Therefore, as a result of the synthetic strategy employed, **1** and **2** have been obtained as well-defined symmetrical dinuclear compounds where both metal centers are coordinated to a pyridine (**1**) or pyrazine (**2**) ring and N2 of the triazole moiety (isomer **a** in Figure 2). This is confirmed by the relative simplicity of the ^{1}H NMR spectra. The spectra are very similar to those obtained for the N2 isomers of mononuclear model complexes **5** and **6**.[7] This similarity confirms that N2 coordination is retained in the coupling reaction, and the symmetry of the spectrum furthermore confirms that both metal centers are equivalent. This observation is not unexpected. Earlier studies have shown that the pyridyl- and pyrazyltriazoles are extremely stable under normal synthetic conditions and that isomerization is only observed for protonated complexes. Deprotonated complexes were found to be photostable.[4e] Both compounds are isolated fully deprotonated, and the protonated species are obtained in situ by the addition of the appropriate amount of acid (Table 1).

Both **1** and **2** exhibit absorption and emission properties, which are characteristic for triazole based ruthenium polypyridyl complexes[4,5] (Table 1). For **1** and its protonated species, the emissive state can be assigned as a bpy based ^{3}MLCT state.[4,5] $\mathbf{H_21}$ emits weakly at 630 nm in acetonitrile, and its emission lifetime is significantly shorter (<5 ns) than that observed for **H1** and **1** (Table 1). The dramatic reduction in emission lifetime is related to the increase in the energy of the luminescent ^{3}MLCT state upon double protonation of the "spectator" bridging ligand and to the simultaneous decrease in the σ-donor strength of the 1,2,4-triazole moiety. This results in a lowering in the energy of the ^{3}MC level, which is known to deactivate the luminescent ^{3}MLCT state by a thermally activated surface crossing process.[2a,7] Somewhat surprisingly, **H1** has an increased emission lifetime. While the luminescent ^{3}MLCT state is undoubtedly raised in energy, it appears that the decrease in the σ-donor strength of the 1,2,4-triazole moieties in **H1** is not as significant as for $\mathbf{H_21}$ or the mononuclear analogue **H5**. As a result, the energy between the ^{3}MLCT and ^{3}MC levels is not sufficiently reduced to allow for more efficient deactivation of the emissive ^{3}MLCT excited state via population of the non-emissive ^{3}MC state. Consequently, the prolonged lifetime of the emitting state of **H1** compared with **1** can be attributed to the energy gap law.[17]

For **2**, the situation is more complex as the effect of protonation is to increase the emission lifetime with a small red shift in emission energy of the order of 10 nm. The difference in luminescence properties of the pyridine (**1** and **5**) and pyrazine (**2** and **6**) based complexes has been attributed to the switching of excited-state localization upon protonation, from a bpy based excited state to a pyrazine based excited state in the case of pyrazine based complexes.[7] Because the acceptor orbitals of the MLCT emitting level(s) in nonprotonated and protonated species of **2** are significantly different, no direct comparison can be made. Luminescence lifetimes for $\mathbf{2}/\mathbf{H2}/\mathbf{H_22}$ are longer than those of the mononuclear complex **6**/**H6**, and this may be indicative of charge delocalization within the dinuclear structures (Table 1).

By comparison with literature data, the oxidation waves at about 1.0 V versus SCE can be assigned as metal centered (Ru^{II}/Ru^{III}) processes.[4,5] Variations in the potential values of the various complexes may be explained on the basis of differences in the donor/acceptor properties of the ligands (Table 1). The oxidation processes of **2** occur at more positive potential than that of **1**, because of the better π-acceptor properties of the pyrazine ring. It is immediately apparent that for both **1** and **2** first metal oxidation potentials are very close to those of monomers **5** and **6**, respectively, and at much lower potential than those of the dinuclear complexes **3** and **4**. The presence of two metal based oxidation processes for both deprotonated and monoprotonated species indicates the presence of a significant intramolecular communication. This is discussed in more detail in the next section.

Intramolecular Interactions. The spectroscopic and electrochemical data discussed previously provide direct

(14) Fennema, B. D. J. R.; Hage, R.; Haasnoot J. G.; Reedijk, J. *J. Chem. Soc., Dalton Trans.* **1990**, 2425.
(15) Tiecco, M.; Tingoli, M.; Testaferri, L.; Chianelli, D.; Wenkert, E. *Tetrahedron* **1986**, *42*, 1475.
(16) Krüger, C.-F.; Miethchen, R. *Chem. Ber.* **1967**, *100*, 2250.
(17) Caspar, J. V.; Kober, E. M.; Sullivan, B. P.; Meyer, T. *J. Am. Chem. Soc.* **1982**, *104*, 630.

Table 2. Spectroelectrochemical Data for Complexes **1**−**4** in 0.1 M TEAP/Acetonitrile

	$\Delta E \pm$ 10 mV	K_c	$\Delta\nu_{1/2}$calcd (cm^{-1})	$\Delta\nu_{1/2}$ (cm^{-1})[b]	ϵ_{max} (M^{-1} cm^{-1}) ± 20%	$E_{op} \pm$ 100 cm^{-1}	α^2
1	180	1100	3060	4690	1820	5490	0.007
H1	110	72	4250	5600	1000	8700	0.0025
2	170	750	3120	4360	1120	5580	0.004
H2	60	10	4300	5300	1000	8500	0.0025
3[a]	300	117910	3341	3300	2400	5556	0.016
4[a]	300	117910	3260	4200	2200	5405	0.019

[a] Taken from ref 6. [b] Taken as double the width at half maximum of the high energy side of the absorption band.

evidence for communication between the two metal centers. They also indicate that this interaction is strongly dependent on the protonation state of the bridging ligand. The presence of two protonation steps with different pK_a values provides further confirmation of this. The effect of communication on the emission behavior is most clearly demonstrated for **H1** (Figure 5) and **H2**. In the absence of any interaction, two emission signals are expected for a monoprotonated species. For **H1**, where the emission energy values expected for the deprotonated (690 nm) and protonated species (630 nm) are significantly different, this would be particularly straightforward to detect. Instead, a single-exponential decay of the emitting state is observed, and the emission at 660 nm is intermediate between that of **1** and $\mathbf{H_2}$**1**. This indicates the presence of a new emitting species, in which the effect of monoprotonation is shared by both metal centers.

Electrochemical and spectroelectrochemical studies can be used to quantify this interaction. The first parameter of interest is the separation between the two metal based oxidation processes (ΔE). This separation is related to the stability of the intervalence compound Ru(II)Ru(III) as defined in eq 1[18]

$$K_c = \exp(\Delta E/25.69) \tag{1}$$

where K_c is the comproportionation constant as defined in eq 2

$$Ru^{II}Ru^{II} + Ru^{III}Ru^{III} \overset{K_c}{\rightleftharpoons} 2Ru^{II}Ru^{III} \tag{2}$$

The ΔE values obtained for the deprotonated compounds of 180 mV for **1** and 170 mV for **2** are indicative of a significant intramolecular communication (Table 2). This interaction is, however, less than that observed for **3** and **4**, for which values of about 300 mV were obtained. For **H1** and **H2**, the difference between first and second metal oxidation waves decreases to 110 mV for **H1** and 60 mV in **H2**. This leads to significantly reduced K_c values indicating a decreased interaction. This decrease in interaction upon protonation is even more prevalent for both $\mathbf{H_2}$**1** and $\mathbf{H_2}$**2** for which only a single two-electron oxidation wave is observed. This indicates that for the fully protonated species K_c is less than 5 and that a mixed valence species does not form in detectable amounts.

More detailed information about the nature of this interaction can be obtained from spectroelectrochemical investigations. On the basis of the electrochemical results outlined previously, intervalence bands can be expected for the deprotonated and the singly protonated species. Analysis of the spectroscopic properties of the intervalence band allows for the estimate of the interaction parameter (α^2) as in eq 3[19]

$$\alpha^2 = \frac{(4.2 \times 10^{-4})\epsilon_{max}\nu_{1/2}}{d^2 E_{op}} \tag{3}$$

where ϵ_{max} is the extinction coefficient of the IT band (M^{-1} cm^{-1}), $\Delta\nu_{1/2}$ is its peak width at half-height, d is the estimated metal to metal distance, 9.5 Å for these compounds, and E_{op} is the energy of the absorption maximum of the intervalence band. Additional information can be obtained by estimating the theoretical peak width at half-height, $\Delta\nu_{1/2calcd}$ using eq 4.[19]

$$\Delta\nu_{1/2calcd} = [2310(E_{op} - \Delta E)]^{1/2} \tag{4}$$

If the value of $\Delta\nu_{1/2}$ obtained from this equation correlates well with the value found from direct measurement, then the system can be described as valence localized $Ru^{II}Ru^{III}$, that is, Type II. If the IT band is narrower then the system, it is better described as type III (valence delocalized).[20] The values obtained from eqs 1−4 are presented in Table 2. On the basis of these data and, in particular, because $\Delta\nu_{1/2}$ observed is larger than $\Delta\nu_{1/2calcd}$, it seems clear that the mixed valence compounds behave as type II (or valence trapped) dinuclear species. Another important observation is that the ΔE, E_{op}, and α^2 values obtained for **1** and **2** are the same within experimental error (Table 2). This observation and the similarity of the energies of the LMCT bands observed for the mixed valence compounds indicate that LUMO of the bridging ligand plays at best minor roles in determining intercomponent interaction. Instead, it is expected that interaction between the metal centers is taking place via a hole transfer mechanism involving the HOMO of the metal units and bridging ligand.[6] This is confirmed by the decrease in interaction observed upon protonation of the bridging ligand. In a hole transfer mechanism, the extent of the interaction depends on the energy gap between the dπ-metal orbitals (metal based HOMO) and the σ-orbitals of the bridge.[21] The spectroscopic and electrochemical data show that the ligand based σ-orbitals are stabilized upon protonation, so that the energy gap between the relevant orbitals *increases*, leading to *decreased* superexchange-assisted electronic interactions.

The α^2 values given in Table 2 indicate that the amount of electron delocalization in **1** and **2** is considerably less than that observed in **3** and **4**. This observation can be explained

(18) Richardson, D. E.; Taube, H. *Inorg. Chem.* **1981**, *20*, 1278.

(19) (a) Hush, N. S. *Prog. Inorg. Chem*. **1967**, *8*, 391. (b) Hush, N. S. *Electrochim. Acta* **1968**, *13*, 1005.

(20) Robin, M. P.; Day, P. *Adv. Inorg. Chem. Radiochem*. **1967**, *10*, 247.

(21) (a) Giuffrida, G.; Campagna, S. *Coord. Chem. Rev.* **1994**, *135*−*136*, 517. (b) Laye, R. H.; Couchman, S. M.; Ward, M. D. *Inorg. Chem.* **2001**, *40*, 4089 and references therein.

by considering the difference in the distance between the two metal centers. Crystallographic data have shown that *d* in **3** is 6.5 Å, while preliminary molecular modeling suggests that in **1** and **2** this distance is 9.5 Å. An additional factor may be that in **3** and **4** the negative charge of the bridge is shared between the two metal centers, while in **1** and **2** the triazole based negative charge is expected to be more localized.

Finally, the difference in the redox and luminescence properties of the deprotonated (**1** and **2**), monoprotonated (**H1** and **H2**), and the diprotonated ($\mathbf{H_2}$**1** and $\mathbf{H_2}$**2**) species warrants some additional comments. On looking at Table 1 and Figure 5, it is clear that the luminescence output of **1** can be switched between three "states" in terms of emission energy and lifetime. It should be stressed, however, that the excited-state responsible for the emission remains the same in all three cases. So, the behavior observed cannot be explained by a switching process between different electronic states. It is rather a stepwise protonation, which perturbs the emitting excited state in such a way that three different outputs are generated. In principle, the same also occurs for **2**; however, the changes in luminescence energy are almost negligible. While the switching of the luminescence output between two "states" is common,[12] the possibility of switching luminescence between three different outputs is less so. In addition, the redox properties of both compounds can also be employed in this respect. For example, by monitoring of the current at 0.8, 1.05, and 1.15 V, the protonation state of **1** may be "read". In view of the future development in the design of systems capable of manipulating information (e.g., light or electrons) at the molecular level, our results offer new lines toward this goal, in terms of both synthetic methods and physical properties.

Conclusions

With the ever-increasing interest in multinuclear metal complexes as supramolecular systems, the assemblies investigated are becoming ever more complex. As a result, the formation of isomers and side products is an increasing problem. The Ni(0) catalyzed homonuclear coupling reported in this contribution is simple and leads to pure compounds in a high yield, in cases where direct reaction of the bridging ligand with the metal centers leads to a mixture of products.[22] To the best of our knowledge, this is the first time such a coupling has been carried out with ruthenium(II) polypyridyl complexes.[8] The method can be adapted to many other systems and constitutes, therefore, together with some related methods,[23] an important tool for the design of novel supramolecular assemblies.

The electrochemical and photophysical studies of the dinuclear compounds obtained illustrate the "tunable nature" of the properties of these supramolecular systems and their potential as molecular switches. The close proximity of the two triazole rings creates interaction between the two parts of the molecule, and the three protonation states obtained show different levels of intercomponent interaction. It is, furthermore, important to note that while the differences in ground-state properties and metal−metal interaction between the pyridine (**1**) and pyrazine (**2**) based complexes are minor, their luminescence properties are substantially different. Relatively small changes in the composition of the compounds, that is, pyridine versus pyrazine, lead to compounds with different excited-state properties. Taking into account the synthetic procedures used in this investigation, this opens the possibility for extensive variation in the components that can be used to build up a range in proton gated redox active and emitting compounds.

Acknowledgment. The authors thank Mr. Maurice Burke and Mr. Michael Burke of Dublin City University for assistance in Mass Spectrometry and ^{1}H NMR spectroscopy. The authors thank MURST (Progetto Artificial photosynthesis), CNR, Enterprise Ireland, and the EU, TMR Grant 96CT-0031, for financial assistance.

IC0112894

(22) Müller, E.; Nazeeruddin, Md. K.; Graetzel, M.; Kalyanasundaram, K.; Prome, J.-C. *New J. Chem*. **1996**, *20*, 759.

(23) (a) Tzalis, D.; Tor, Y. *J. Am. Chem. Soc.* **1997**, *119*, 852. (b) Connors, P. J., Jr.; Tzalis, D.; Dunnick, A. L.; Tor, Y. *Inorg. Chem*. **1998**, *37*, 1121. (c) Chodorowski-Kimmes, S.; Beley, M.; Colin, J.-P.; Sauvage, J.-P. *Tetrahedron Lett*. **1996**, *37*, 2963. (d) Dunne, S. J.; Constable, E. C. *Inorg. Chem. Commun.* **1998**, *1*, 167. (e) Johansson, K. O.; Lotoski, J. A.; Tong, C. C.; Hanan, G. S. *Chem. Commun.* **2000**, 819. (f) Griffiths, P. M.; Loiseau, F.; Puntoriero, F.; Serroni, S.; Campagna, S. *Chem. Commun.* **2000**, 2297.